

Spontaneous Curvature Induced Shape Transformations of Tubular Polymersomes

W. T. Gózdź

*Institute of Physical Chemistry, Polish Academy of Sciences,
Kasprzaka 44/52, 01-224 Warsaw, Poland*

Received January 24, 2004. In Final Form: May 12, 2004

The behavior of tubular polymersomes is investigated within the framework of the elastic energy model. The transition from a cylindrical tube to a chain of beads connected by small necks is studied in detail. The evolution of a polymersome shape, resulting from a change of the temperature is modeled by the shape transformations caused by a change of the spontaneous curvature. Good agreement between the experiments and the theoretical calculations is found.

1. Introduction

It has been demonstrated experimentally that tubular polymersomes^{1,2} undergo a shape transition, induced by lowering the temperature, from a cylinder to a chain of connected beads.³ The transition takes place for the elongated polymersomes of varying length and diameter. Such shapes are formed in the region of the phase diagram, where the reduced volume is low and the spontaneous curvature is high. This region was not fully explored theoretically, in contrast to the region of large reduced volume and small spontaneous curvature.⁴ Similar transformations of bilayer membranes which form cylindrical shapes into beads are often encountered in biological systems. The transformations are induced by different stimuli. For example, the action of laser tweezers^{5–7} or the presence of hydrophilic polymers with hydrophobic side groups^{8,9} induce the transformations from cylinders to beads. The laser tweezers touching a membrane surface exert some tension on the membrane, which results in the formation of peristaltic shapes on the cylindrical membrane. This phenomenon is called pearling instability. Polymers attached to a membrane may induce the spontaneous curvature, which results in a change of the membrane shape. Pearling of a tubular protrusion may also happen after destruction of a microtubules which generated such a protrusion.¹⁰ The results of experiments published in ref 3 suggest that the shape transformation, induced by a change of the temperature, may result from a change of the spontaneous curvature. In this paper such a hypothesis is studied in detail by comparing the experimental results published in ref 3 with the numerical calculations based on the elastic energy model. Such a dependence of the temperature and the spontaneous

curvature has been observed in the behavior of high genus polymersomes.¹¹ It is thus plausible that a similar relation between the temperature and the spontaneous curvature exists in other cases, but this assumption requires further verification.

The ensemble which mimics the experimental situation is one with constant surface area S and volume V of a polymersome, since the bilayer membrane is hardly stretchable and the experiment was performed at isotonic conditions. It is also assumed that a temperature change induces a change of the spontaneous curvature. Such a physical situation is well described by the elastic energy^{12–14} given by

$$\mathcal{F} = \frac{\kappa}{2} \int_S dS (C_1 + C_2 - C_0)^2 \quad (1)$$

where κ is the bending rigidity, C_1 and C_2 are the principal curvatures, C_0 is the spontaneous curvature, and the integral (1) is taken over the surface of a closed vesicle. No topology changes are assumed; therefore the integral over the Gaussian curvature contributes a constant value and is omitted in eq 1. The functional (1) is scale invariant; thus the equilibrium shapes do not depend on the actual size of vesicles. To mimic the experimental conditions, the constraints of constant surface area S and volume V of a polymersome are imposed. In this paper I am comparing the shape profiles resulting from numerical calculations with experimental pictures to find a correspondence between theoretical parameters and experimental conditions. The existence of such a correspondence may support the hypothesis that a temperature change induces a change of the spontaneous curvature.

2. Parametrization

The shapes of the polymersomes observed in experiments exhibit rotational symmetry and have mirror symmetry with respect to the plane perpendicular to the

- (1) Disher, B. M.; et al. *Science* **1999**, *284*, 1143.
- (2) Discher, D. E.; Eisenberg, A. *Science* **2002**, *297*, 967.
- (3) Reinecke, A. A.; Doebereiner, H.-G. *Langmuir* **2003**, *19*, 605.
- (4) Seifert, U.; Berndl, K.; Lipowsky, R. *Phys. Rev. E* **1990**, *44*, 1182.
- (5) Bar-Ziv, R.; Moses, E. *Phys. Rev. Lett.* **1994**, *73*, 1392.
- (6) Bar-Ziv, R.; Moses, E.; Nelson, P. *Biophys. J.* **1998**, *75*, 294.
- (7) Nelson, P.; Powers, T.; Seifert, U. *Phys. Rev. Lett.* **1995**, *74*, 3384.
- (8) Tsafirir, I.; et al. *Phys. Rev. Lett.* **2001**, *86*, 1138.
- (9) Tsafirir, I.; et al. *Phys. Rev. Lett.* **2003**, *91*, 138102.
- (10) D'Onofrio, T. G.; et al. *Langmuir* **2003**, *19*, 1618.

- (11) Haluska, C. K.; et al. *Phys. Rev. Lett.* **2002**, *89*, 238302.
- (12) Helfrich, W. *Z. Naturforsch.* **1973**, *28 c*, 693.
- (13) Evans, E. *Biophys. J.* **1974**, *14*, 923.
- (14) Canham, P. B. *J. Theor. Biol.* **1970**, *26*, 61.

rotational axis, located in the middle of the polymersomes. Vesicle shapes can be well approximated in numerical calculations by surfaces which are rotationally symmetric. Therefore, the tubular vesicles can be studied by parametrizing their shape with the angle between the rotation axis and the line tangent to the shape profile, $\theta(s)$, as a function of the arclength s . The radius $r(s)$ and the height $z(s)$ of the shape profile are calculated from $\theta(s)$ according to

$$r(s) = \int_0^s ds' \cos(\theta(s')) \quad (2)$$

$$z(s) = \int_0^s ds' \sin(\theta(s')) \quad (3)$$

To parametrize a closed shape, the following boundary conditions must also be satisfied:

$$\theta(0) = 0 \quad (4)$$

$$\theta(L_s) = \pi \quad (5)$$

$$r(L_s) = 0 \quad (6)$$

where L_s is the length of the shape profile. Equations 4 and 5 guarantee that the profile is smooth at the ends, and eq 6 accounts for the fact that the vesicle is closed.

The functional (1) with the shape profile parametrized by $\theta(s)$ is given by

$$\mathcal{F} = \frac{\kappa}{2} (2\pi) \int_0^{L_s/2} ds r(s) \left(\frac{d\theta(s)}{ds} + \frac{\sin(\theta(s))}{r(s)} - C_0 \right)^2 \quad (7)$$

The derivation of the expressions for the principal curvatures is given in the Appendix. In the numerical calculations, I exploit the fact that the shape profile is symmetric with respect to the plane perpendicular to the rotation axis. In such a case only two boundary conditions are needed, the first is the same as in eq 4 and the second is

$$\theta(L_s/2) = \pi/2 \quad (8)$$

The functional (7) is minimized numerically. The function describing the shape profile $\theta(s)$ is approximated by the Fourier series, eq 9

$$\theta(s) = \theta_0 \frac{s}{L_s} 2 + \sum_{i=1}^N a_i \sin\left(\frac{2\pi}{L_s} is\right) \quad (9)$$

where N is the number of Fourier modes and a_i are the Fourier amplitudes. θ_0 is the angle at the middle of a vesicle, $\theta_0 = \theta(L_s/2)$. The functional minimization is replaced by the minimization of the function of many variables. The functional (7) is minimized with respect to the amplitudes a_i and the length of the shape profile L_s , under the constraint of constant surface area S and volume V , where

$$S = 2\pi \int_0^{L_s/2} ds r(s) \quad (10)$$

$$V = \pi \int_0^{L_s/2} ds r^2(s) \sin \theta(s) \quad (11)$$

A large number of amplitudes, on the order of 100, is required in order to accurately parametrize complex shapes.

The volume, V_0 , and the radius, R_0 , of the sphere having the same surface area, S , as the investigated vesicle are chosen as the volume and length units respectively.^{4,15}

$$R_0 = (S/4\pi)^{1/2} \quad (12)$$

$$V_0 = \frac{4}{3} \pi R_0^3 \quad (13)$$

The dimensionless, reduced volume v and the dimensionless spontaneous curvature c_0 are defined as

$$v = V/V_0 \quad (14)$$

$$c_0 = C_0 R_0 \quad (15)$$

Thus, there are only two control parameters important for the process, v and c_0 , since the model is scale invariant. If the reduced volume is set constant, the only remaining free parameter is the spontaneous curvature c_0 .

3. Results and Discussion

The main purpose of this section is to examine the influence of the spontaneous curvature on the conformations of long and short tubular polymersomes, which resemble the polymersomes studied experimentally in ref 3. It has to be noted that in ref 3 a change of the shapes of polymersomes is due to a nonequilibrium process which is the result of a rapid temperature change. In this paper equilibrium shape profiles are calculated. Nevertheless, I believe that it is possible to gain significant insight into the nonequilibrium dynamics by analyzing the results of the equilibrium theory.

The viscosity coefficient for polymersome membranes is 500 times larger than the viscosity coefficient for lipid membranes.¹⁶ The large viscosity indicates that the relaxation dynamics is slow and may proceed through a series of metastable states, as suggested in ref 3. It is assumed that a temperature change does not lead to an immediate change of the spontaneous curvature. The spontaneous curvature changes gradually and the shape of the membrane is adjusted to slow gradual changes of the spontaneous curvature. One can speculate that instantaneous stages of the slow relaxation process are very similar to some equilibrium states. These metastable states can be identified with the minima of the functional 7. This hypothesis is examined in this section.

The behavior of long and short polymersomes is described in sections 3.2 and 3.3. In section 3.1, the more general case, where the reduced volume is unconstrained, is studied first as a complementary example. Comparison of these three cases shall give a more complete picture of the studied problem.

3.1. Unconstrained Volume. Shapes of vesicles are governed by the reduced volume and the spontaneous curvature. To distinguish the role of the spontaneous curvature and the reduced volume in the process of shape transformations, I start by examining the case where the surface area S of a polymersome is constant and the volume V is unconstrained. Such a situation may hypothetically happen when a membrane is ideally permeable. Thus, the shape transformations are driven only by a change of the spontaneous curvature C_0 . It is obvious that when the dimensionless spontaneous curvature c_0 is equal to 2, the shape minimizing the functional (1) is a sphere and the

(15) Miao, L.; Fourcade, B.; Rao, M.; Wortis, M. *Phys. Rev. A* **1991**, *43*, 6843.

(16) Dimova, R.; et al. *Eur. Phys. J. E* **2002**, *7*, 241.

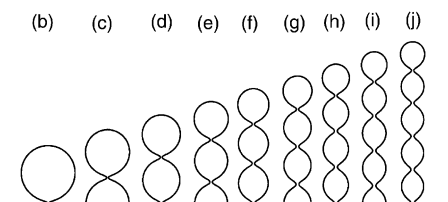


Figure 1. The profiles calculated for a constant surface area and different spontaneous curvature. The configurations with the minimal energy for a given number of beads are shown. No volume constraint is applied. The dashed line denotes the symmetry plane, only half of the vesicle is shown. The calculations were performed for 160 Fourier amplitudes.

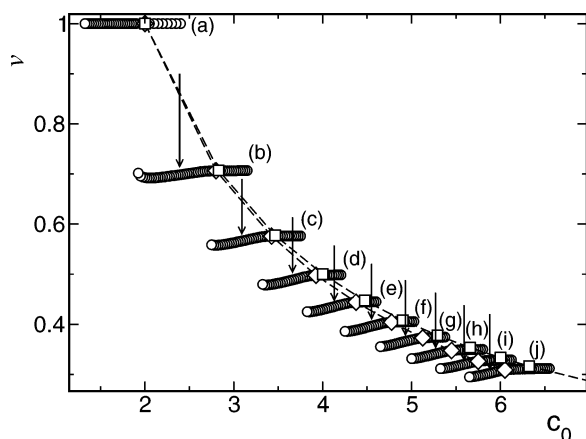


Figure 2. Reduced volume of tubular polymersomes, $v = V/V_0$, versus the dimensionless spontaneous curvature, $c_0 = C_0 R_0$. Open circles denote the results of minimization without a volume constraint. Open squares represent configurations composed of touching spheres, with different numbers of spheres and the same total surface area. Open diamonds denote the configurations with minimal energy from Figure 1. The calculations were performed for 160 Fourier amplitudes. The dashed lines are added as a guide to the eye.

bending energy is zero, since each principal curvature (C_1 , C_2) equals 1 at every point of the surface. Increasing the spontaneous curvature beyond $c_0 = 2$ results in a series of transitions in which the sphere is transformed into chains of beads connected by small necks, as shown in Figure 1. The size, the number, and the shape of the beads are governed by the spontaneous curvature. The transitions are discontinuous, which can be easily seen from the plots of the volume of the polymersomes as a function of the spontaneous curvature. The reduced volume $v = V/V_0$ as a function of the dimensionless spontaneous curvature $c_0 = C_0 R_0$ is presented in Figure 2. The lines of open circles denoted by letters from (a) to (j) in Figure 2 show the values of v and c_0 for which a minimum of the functional (7) was found. The letter (a) represents the minima for spheres, (b) for dumbbells, (c) for tree-bead vesicles, and so on as indicated in Figure 1. The minima of the functional are either global or local, since for the same parameters more than one solution is found. Comparing the curvature energy as a function of the spontaneous curvature for two configurations which differ by one bead, one finds the value of the spontaneous curvature for which the energies for the two configurations are equal. These values are marked by vertical arrows in Figure 2. At these values the configurations with a larger number of beads become global minima while the configurations with a smaller number of beads become local minima. The value of equal energy is the highest for the pair of configurations with the smallest number of beads, i.e., for spheres and dumbbells, because the difference in

shape, and therefore in the reduced volume, is the largest for the configurations with a smaller number of beads. The value of equal energy for pairs of configurations with n and $n + 1$ beads decreases when n is increased. It indicates that the shape transitions involving a change of the number of beads is easier for configurations with a large number of beads, which are stable at low reduced volume.

The first point at each branch, starting from the left side, marks the boundary of stable solutions obtained from the minimization of the functional (7); i.e., on a given branch, there are no solutions with a number of beads characteristic for this branch for smaller values of c_0 . An exception is the spherical configuration, for which a solution can be found for any value of the spontaneous curvatures in the range presented in Figure 2. The values of the spontaneous curvature for end points on the right side of each branch were arbitrarily chosen, when the shape of the configurations weakly changes with the increase of the spontaneous curvature. The reduced volume decreases with the decrease of the dimensionless spontaneous curvature, for a configuration with a given number of beads, due to widening of the necks. When the volume is unconstrained, configurations resembling cylinders are never stable or even metastable. The shapes of polymersomes usually resemble a chain of beads connected by narrow necks. These shapes are similar to the shapes of buds which are formed from domains of one component in two components membranes under weak tension in the strong segregation limit.¹⁷ The decrease of the spontaneous curvature results in widening the necks of a configuration with a given number of beads in such a way that all the necks become wider simultaneously. Thus by monitoring the width of the necks, it is possible to monitor a change of the spontaneous curvature C_0 . The direction of a change of the spontaneous curvature can be also predicted. The knowledge of such a dependence between the shape of a polymersome and the spontaneous curvature may be helpful in interpretation of experimental results.

3.2. Long Polymersomes. The volume constraint changes significantly the behavior of the tubular polymersomes. In an ensemble of constant surface area S , volume V , and spontaneous curvature C_0 , the configurations which resemble cylinders closed at the ends by hemispheres, become stable. Such configurations are in fact observed in experiments.³ It has been shown that by decreasing the temperature the shape transition from a cylinder to a chain of beads is induced.³ The formation of beads starts simultaneously from both ends of a tubular polymersome and continues toward the center until the beads occupy the entire length of the polymersome. On the basis of the experimental results, one may speculate that formation of beads indicates that a change of the temperature induces a spontaneous curvature change. It may be possible to guess the values of c_0 by mapping the shape profiles of polymersomes from numerical calculations to pictures from experimental observations.

The experimental results from ref 3 are reported in detail for two types of tubular polymersomes of different length. They can be characterized by the number of beads: the first with 16 beads and the second with 6 beads. The reduced volume, v , of the polymersomes investigated in the numerical calculations was chosen by trial and error method to reproduce the configurations with the same number of beads as those in the experiments. The reduced volume $v = 0.235$ was estimated for the longer polymer-

(17) Gózdź, W. T.; Gompper, G. *Europhys. Lett.* **2001**, *55*, 587.

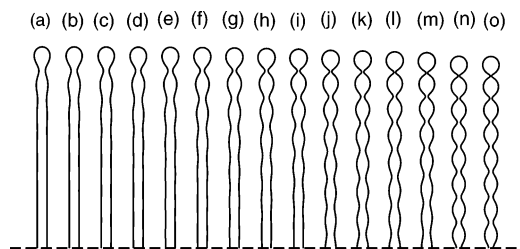


Figure 3. Shape transformation of a long tube induced by the change of the spontaneous curvature. Only the upper half of the shape profile is shown since it is symmetric with respect to the horizontal axis. Reduced volume v is set to 0.235. The calculations were done for 320 Fourier modes. The spontaneous curvature c_0 is (a) 6.05, (b) 6.15, (c) 6.25, (d) 6.35, (e) 6.45, (f) 6.55, (g) 6.65, (h) 6.75, (i) 6.85, (j) 6.95, (k) 7.05, (l) 7.15, (m) 7.25, (n) 7.35, and (o) 7.45.

some with 16 beads. It has been observed that the exact number of beads is not crucial for the behavior of the long polymersomes. The long polymersomes which can be obtained for different, small values of the reduced volume behave in a similar way. The region of the phase diagram where long tubular vesicles are stable (characterized by low reduced volume and high spontaneous curvature) has not been studied in detail. The research has focused mainly on the region of low c_0 and large or moderate v .^{4,15}

The shape evolution driven by a change of the spontaneous curvature, calculated numerically for the long polymersome, $v = 0.235$, is shown in Figure 3. For low values of the spontaneous curvature, c_0 , the polymersome is mainly cylindrical, as is shown in configurations (a–f) in Figure 3. Increasing the spontaneous curvature induces the beading process. The formation of beads begins at the ends and proceeds gradually toward the center, exactly as it has been observed in the experiment. The beads have approximately the same size. Thus, by changing only the spontaneous curvature while keeping constant surface area and volume, the transition observed in the experiments can be reproduced. Such a behavior suggests possible mechanism of the transformation. The change of the temperature induces gradual change of the spontaneous curvature, from the equilibrium value characteristic for a cylinder to the equilibrium value characteristic for beads.

For the long polymersome, a morphological transition has been observed, in which the number of beads increases in the polymersome already covered with beads on its whole length. This transition is discontinuous, which can be seen by looking at the configurations (m) and (n) in Figure 3. Configuration (m) in Figure 3 is build of 15 beads, which are more pronounced at the ends and less pronounced in the middle. When the spontaneous curvature is increased, then the new configuration with 15 beads becomes metastable and next a solution with 16 beads no longer exists. There exists only a solution with 16 pronounced beads as presented in the configuration (n), but there is no continuous transition from a configuration with 15 beads to 16 beads at least in the situation modeled here. Such a transition exists also for long polymersomes with different number of beads other than in the polymersome studied in detail in this paper.

The curvature energy is lowered during the formation of beads and is the lowest when the whole polymersome is composed of beads as shown in Figure 4. The elastic energy is measured in units of the bending energy of a sphere ($8\pi\kappa$). Two types of shape transitions can be distinguished by examining the dependence of the elastic energy on the spontaneous curvature for the long polymersome: the first one, continuous transition from cy-

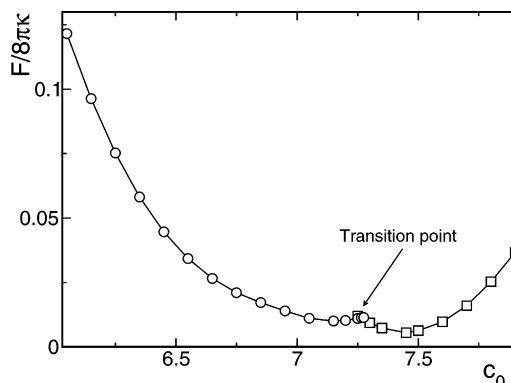


Figure 4. The elastic energy as a function of the reduced spontaneous curvature for the long polymersome obtained for the reduced volume $v = 0.235$. The calculations were done for 320 Fourier modes. The lines are added to guide the eye. The open circles represent the evolution of the polymersome from the cylinder to the configuration with 15 beads. The open squares represent the configurations with 16 beads.

lindrical polymersome to beads, configurations from (a) to (m); the second one, discontinuous transition, when the number of beads is changed from 15 beads in configuration (m) to 16 beads in configuration (n).

Two different curves can be distinguished on the plot of the elastic energy as a function of the spontaneous curvature. The first curve which begins at $c_0 = 6.0$ and ends at $c_0 = 7.275$ represents the elastic energy change for the continuous transformation from cylindrical polymersome to the one composed of 15 beads. The second curve which begins at $c_0 = 7.25$ represents the energy change for the polymersome composed of 16 beads. Two minima of the functional (7) were found at $c_0 = 7.25$. The global minimum is marked by an open circle, the local one is marked by an open square in Figure 4. These two minima represent two families of shapes with 15 beads and with 16 beads. The range of the spontaneous curvature, for which two solutions are found, is small. The intersection point of these two curves marks the discontinuous transition. The shape of the polymersomes composed of 16 beads does not change significantly with the change of the spontaneous curvature. Each energy curve has a minimum for a different value of c_0 . The minima are close to the intersection point of the energy curves. The energy at the minimum is lower for the configuration with 16 beads, suggesting that it should be more common in nature. Near the intersection point, the energies have two values for the same values of c_0 and v , which represent stable and metastable solutions resulting from minimization of the functional (7). These are the solution for the polymersomes with 15 and 16 beads. Thus, hysteresis effects may be expected.

It is shown in Figure 5 that the width of the first neck decreases roughly linearly with the spontaneous curvature during the shape transformation. The same tendency has been observed in the experiments. It should be noted that the neck radius changes significantly with the spontaneous curvature only for the shape transformation from cylindrical polymersome to the one composed of 15 beads. The whole shape, and particularly the neck radius, does not change significantly for the polymersome composed of 16 beads. A change of the spontaneous curvature induces a change of a vesicle shape and therefore a change of the distribution of the mean curvature on the vesicle surface. The mean curvature is distributed more uniformly on the vesicle when the neck radius decreases; i.e., the difference in the mean curvature at the ends and the center of the vesicle decreases.

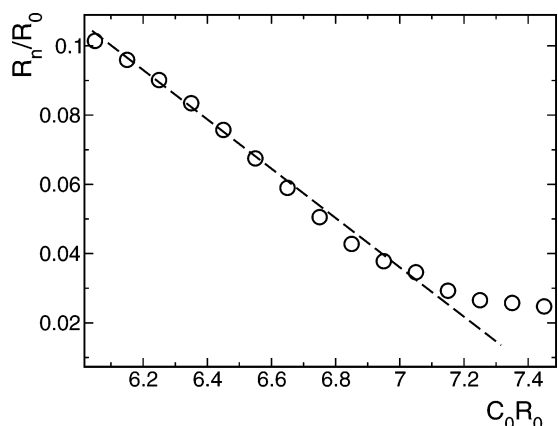


Figure 5. The radius of the first neck closest to the ends, R_n , as a function of the spontaneous curvature for the long polymersome, obtained for the reduced volume $\nu = 0.235$. The dashed line is added as a guide to the eye. The calculations were done for 320 Fourier modes.

3.3. Short Polymersomes. It can be inferred from the calculations for unconstrained volume that the configurations with six beads are stable for the range of values of the reduced volume, $0.386 < \nu < 0.408$. The lower bound $\nu = 0.386$ is the reduced volume of the stable configuration with the smallest spontaneous curvature $c_0 = 0.425$. The upper bound is the volume of touching spheres, for which $c_0 = 4.899$. The configuration with the lowest energy, shown in Figure 6A, was calculated for $c_0 = 4.775$ and has the reduced volume $\nu = 0.404$ for 160 Fourier modes. The shape evolution has been studied for three different values of the reduced volume $\nu = 0.38$, $\nu = 0.39$, and $\nu = 0.40$.

The profiles calculated numerically for short polymersomes are shown in Figure 6B–D.

Although the shape profiles look similar for different values of the reduced volume, the shape evolution in each case proceeds differently, which can be seen when one examines the plots of the elastic energy, shown in Figure 7. Small differences in the reduced volume may change the transformations induced by the spontaneous curvature. The common feature is the existence of cylindrical configurations for small c_0 and beads for high c_0 .

For $\nu = 0.38$ and for $\nu = 0.40$ the plots of the elastic energy have two minima. Each minimum characterizes different family of shapes. A change of c_0 at constant ν leads to the transition between these two families. The transitions calculated numerically are therefore first order. The hysteresis effect can be observed. The shape profiles which represent the vesicles at the minima of the elastic energy for $\nu = 0.38$ are presented in Figure 6B as configurations B(c) and B(e). Configuration B(c) results from the continuous evolution of the configuration B(a), with intermediate profile B(b). The configuration B(e) represents the shape profile at the second minimum. The configurations B(c) and B(e) are composed of beads, but the number of beads is larger for the configuration B(e). The configuration B(d) is a metastable configuration evolved from B(a) at c_0 where the stable one is the configuration B(e). It should be noted that the reduced volume $\nu = 0.38$ is outside the range of the stable configurations calculated without a volume constraint. Thus, a volume constraint may stabilize certain configurations. The shape profiles which represent the vesicles at the minima of the elastic energy for $\nu = 0.40$ are presented in Figure 6D as configurations D(c) and D(d).

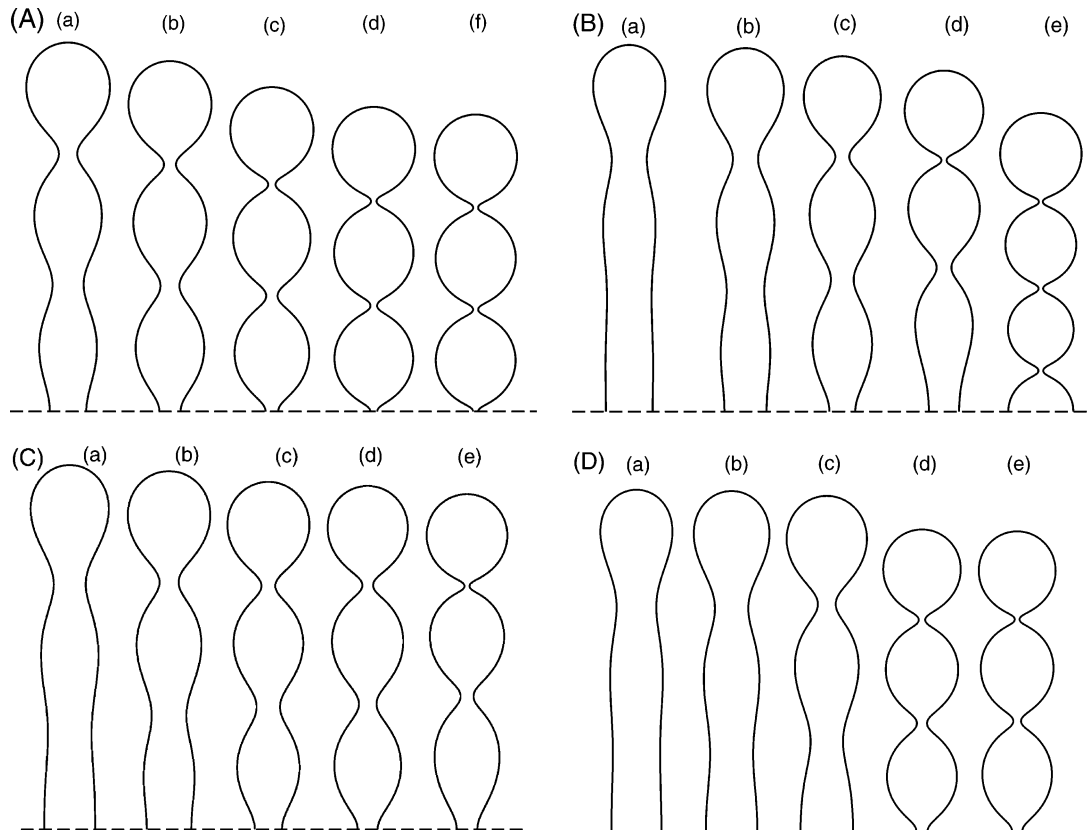


Figure 6. Shape transformation of a short tube induced by a change of the spontaneous curvature. The dashed line shows the symmetry plane, only the upper half of a shape profile is presented. (A) no volume constraint: (a) $c_0 = 4.25$, (b) $c_0 = 4.45$, (c) $c_0 = 4.625$, (d) $c_0 = 4.775$, (e) $c_0 = 5.025$. (B) Reduced volume $\nu = 0.38$: (a) $c_0 = 3.6$, (b) $c_0 = 4.1$, (c) $c_0 = 4.6$, (d) $c_0 = 5.1$, (e) $c_0 = 5.25$. (C) Reduced volume $\nu = 0.39$: (a) $c_0 = 3.8$, (b) $c_0 = 4.25$, (c) $c_0 = 4.30$, (d) $c_0 = 4.65$, (e) $c_0 = 5.25$. (D) Reduced volume $\nu = 0.40$: (a) $c_0 = 3.1$, (b) $c_0 = 3.6$, (c) $c_0 = 4.3$, (d) $c_0 = 4.7$, (e) $c_0 = 5.3$.

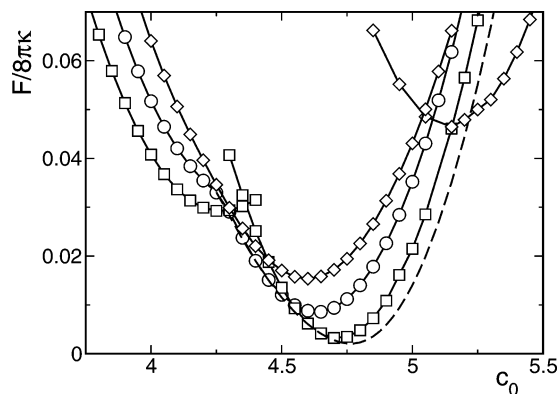


Figure 7. Elastic energy as a function of the spontaneous curvature for short polymersomes obtained for the reduced volumes $v = 0.38$ (diamonds), $v = 0.39$ (open circles), and $v = 0.40$ (open squares). The dashed line denotes the energy of the configurations calculated for unconstrained volume. The calculations were done for 160 Fourier modes.

The configuration D(c) evolved from the configuration D(a), with the intermediate configuration D(b). The configuration at the minimum is still very similar to the initial cylindrical configuration; the beads are not yet pronounced. If the configuration D(c) could evolve further, it would evolve to the configuration with five beads. The configuration D(d) represents the second minimum, it does not change significantly when c_0 is changed as seen in D(e). It is very similar to the configurations A(c), A(d) with unconstrained volume, which can be understood by comparing the plots of elastic energies for $v = 0.40$ and unconstrained v . The plots of elastic energies are close to each other and overlap at an interval near the minimum.

For $v = 0.39$, there is only one minimum; however the plot of elastic energy exhibits an inflection point. The profile at the minimum is pictured as configuration C(d) in Figure 6. The configurations C(b) and C(c) show the profiles before and after the inflection point. At the inflection point the shape profile changes most significantly, but smoothly. For this reduced volume the transition is like a continuous transition.

Having examined these three different scenarios for three values of the reduced volume v , one may better understand the experimental observations. If the energy barrier between the minima is high, the transformation from cylinder to beads may proceed with difficulties, and strong hysteresis effects should be expected. If the energy barrier is small or there is only one minimum, the transformation should be easy, and hysteresis effects should not exist or be negligible. It has been reported in ref 3 that for some polymersomes the beading process started immediately and for others after some period of time.

In experimental systems the area of a bilayer expands with an increase of the temperature. The expression which relates area expansion with the temperature is not known. However, it may be assumed, based on the experimental results, that the area expansion is not significant and may be neglected in the calculations which are to explain the shape transformations studied in this paper. It has to be noted that the relaxation process takes place at constant temperature.

4. Conclusions

The shape transformations of tubular polymersomes were investigated within the framework of the elastic energy model. It has been demonstrated that a change of the spontaneous curvature induces the shape transformations of a cylinder to a chain of beads. The numerical

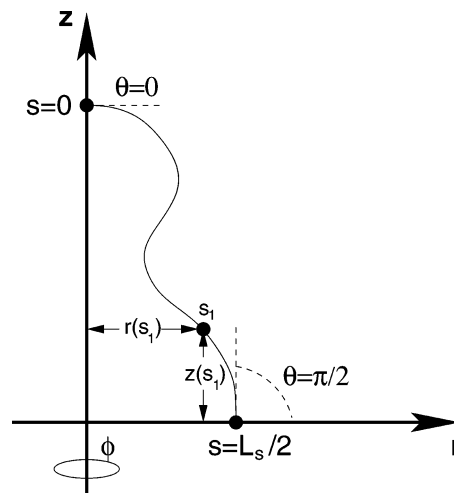


Figure 8. Schematic representation of a profile in the arclength parametrization. The coordinates of the point located at s_1 on the curve are given by $r(s_1)$ and $z(s_1)$. s is the arclength.

calculations reflect the behavior of the tubular polymersomes observed in experiments described in ref 3. It has been confirmed that a change of the temperature results in a change of the spontaneous curvature, which leads to the shape transformations. The first-order shape transition in which the number of beads is changed due to an increase of the spontaneous curvature has been discovered. Such a transition exists for tubular polymersomes of various lengths. The transformation from cylindrical polymersomes to beads is usually accompanied by the discontinuous shape transition. The existence of such a transition suggests the possibility of hysteresis effects in experiments. It has been shown that the straight, cylindrical configurations are stabilized by the volume constraint. A tiny difference in the reduced volume may lead to different evolution of the polymersomes. This may explain the behavior of the polymersomes studied in the experiment, where the transition from cylindrical tubes to beads and vice versa took place for some polymersomes and for the other did not.

Acknowledgment. I would like to acknowledge the support from the Polish State Committee for Scientific Research 1 P03B 033 26.

5. Appendix

5.1. Derivation of the Expressions for the Principal Curvatures. $z(s)$ and $r(s)$ are parametric equations of a curve in the r - z plane, where the parameter is the arclength s .

$$z(s) = \int_0^s \sin(\theta(s')) ds'$$

$$r(s) = \int_0^s \cos(\theta(s')) ds'$$

The function $\theta(s)$ describes the curve. $\theta(s)$ is an angle which is formed by the r -axis and the tangent line to the curve at a point located in a distance s on the curve. ϕ is the angle of rotation around the z -axis. $L_s/2$ is the value of the arclength at the point in which the profile crosses the r -axis. A vector $\mathbf{R} = \{x(\phi, s), y(\phi, s), z(\phi, s)\}$ in the three-dimensional Euclidian space describing the points on a surface of revolution parametrized with the function $\theta(s)$ is given by

$$\mathbf{R} = \{\cos(\phi) r(s), \sin(\phi) r(s), z(s)\}$$

ϕ and s are coordinates on the surface. x , y , and z are coordinates in the three-dimensional Euclidian space. The differential geometry can be used to calculate principal curvatures C_1 and C_2 for the surface.¹⁸

First, the metric tensor g_{ij} is constructed as

$$g_{ij} = \begin{pmatrix} \frac{\partial \mathbf{R}}{\partial s} \cdot \frac{\partial \mathbf{R}}{\partial s} & \frac{\partial \mathbf{R}}{\partial s} \cdot \frac{\partial \mathbf{R}}{\partial \phi} \\ \frac{\partial \mathbf{R}}{\partial s} \cdot \frac{\partial \mathbf{R}}{\partial \phi} & \frac{\partial \mathbf{R}}{\partial \phi} \cdot \frac{\partial \mathbf{R}}{\partial \phi} \end{pmatrix} = \begin{pmatrix} 1 & 0 \\ 0 & (r(s))^2 \end{pmatrix}$$

where

$$\frac{\partial \mathbf{R}}{\partial s} = \{\cos(\phi) \cos(\theta(s)), \cos(\theta(s)) \sin(\phi), \sin(\theta(s))\}$$

$$\frac{\partial \mathbf{R}}{\partial \phi} = \{-\sin(\phi) r(s), \cos(\phi) r(s), 0\}$$

The unit normal \mathbf{n} can be calculated from

$$\mathbf{n} = (\frac{\partial \mathbf{R}}{\partial \phi} \times \frac{\partial \mathbf{R}}{\partial s}) / (\det(g_{ij}))^{1/2} = \{-\cos(\phi) \sin(\theta(s)), -\sin(\phi) \sin(\theta(s)), \cos(\theta(s))\}$$

(18) Stoker, J. Differential Geometry. In *Pure and Applied Mathematics*; Courant, R., Bers, L., Stoker, J., Eds.; Wiley: New York, 1969; Vol. XX.

Define \mathbf{Y} and L_{ij} as

$$\mathbf{Y} = \begin{pmatrix} \frac{\partial^2 \mathbf{R}}{\partial s \partial s} & \frac{\partial^2 \mathbf{R}}{\partial s \partial \phi} \\ \frac{\partial^2 \mathbf{R}}{\partial \phi \partial s} & \frac{\partial^2 \mathbf{R}}{\partial \phi \partial \phi} \end{pmatrix}$$

$$L_{ij} = \mathbf{Y} \cdot \mathbf{n}$$

The H_{ij} tensor is then

$$H_{ij} = g_{ij}^{-1} L_{ij} = \begin{pmatrix} \frac{d\theta(s)}{ds} & 0 \\ 0 & \frac{\sin(\theta(s))}{r(s)} \end{pmatrix}$$

Thus C_1 and C_2 are

$$C_1 = \frac{d\theta(s)}{ds}$$

$$C_2 = \frac{\sin(\theta(s))}{r(s)}$$

LA049776U